Published OnlineFirst December 1, 2009; DOI: 10.1158/0008-5472.CAN-09-1257

Epithelial-to-Mesenchymal Transition and Ovarian Tumor Progression Induced by Tissue Transglutaminase

Minghai Shao,[1] Liyun Cao,[1] Changyu Shen,[1] Minati Satpathy,[1] Bhadrani Chelladurai,[1] Robert M. Bigsby,[2,5] Harikrishna Nakshatri,[3,4,5] and Daniela Matei[1,2,4,5,6]

Departments of [1]Medicine, [2]Obstetrics and Gynecology, [3]Surgery, and [4]Biochemistry and Molecular Biology, [5]IU Simon Cancer Center, and [6]VA Roudebush Hospital, Indiana University School of Medicine, Indianapolis, Indiana

Abstract

Tissue transglutaminase (TG2), an enzyme that catalyzes Ca^{2+}-dependent aggregation and polymerization of proteins, is overexpressed in ovarian cancer cells and tumors. We previously reported that TG2 facilitates tumor dissemination using an i.p. xenograft model. Here we show that TG2 modulates epithelial-to-mesenchymal transition (EMT), contributing to increased ovarian cancer cell invasiveness and tumor metastasis. By using stable knockdown and overexpression in epithelial ovarian cancer cells, we show that TG2 induces a mesenchymal phenotype, characterized by cadherin switch and invasive behavior in a Matrigel matrix. This is mediated at the transcriptional level by altering the expression levels and function of several transcriptional repressors, including *Zeb1*. One mechanism through which TG2 induces *Zeb1* is by activating the nuclear factor-κB complex. The effects of TG2 on ovarian cancer cell phenotype and invasiveness translate into increased tumor formation and metastasis *in vivo*, as assessed by an orthotopic ovarian xenograft model. Highly expressed in ovarian tumors, TG2 promotes EMT and enhances ovarian tumor metastasis by activating oncogenic signaling. [Cancer Res 2009;69(24):9192–201]

Introduction

Tissue transglutaminase (TG2), an enzyme overexpressed in epithelial malignancies (1, 2), participates in Ca^{2+}-dependent protein posttranslational modifications and cross-linking (3). We reported that TG2 is upregulated in ovarian tumors compared with normal ovarian surface epithelium (1, 4). The enzyme exerts pleiotropic functions in tumors. It strengthens integrin-dependent cell adhesion, remodels the extracellular matrix (ECM), and modulates intracellular signaling (5). In cancer cells, TG2 activates focal adhesion kinase, protein kinase B (Akt; ref. 6), cyclic AMP response element binding protein (7), and the nuclear factor-κB (NF-κB) complex (2). Activation of oncogenic signaling affects the invasive behavior of tumor cells. We recently showed that TG2 plays a role in i.p. dissemination of ovarian cancer cells (1) and regulates at the transcription level the secretion of matrix metalloproteinase-2 (MMP-2; ref. 7). To better understand its function in metastasis, we investigated the involvement of TG2 in epithelial-to-mesenchymal transition (EMT), a critical process in cancer progression.

EMT is characterized by breakdown of cell junctions and loss of cell polarity, rendering epithelial cells motile and invasive (8). EMT plays an important role in development, particularly in gastrulation and neural crest migration (9). In cancer, EMT causes cells to lose epithelial characteristics and acquire a mesenchymal phenotype, initiating invasion and metastasis. A critical component is the loss of type I cadherins that maintain stable cell-cell contacts through adherens junctions and desmosomes (10, 11). The extracellular immunoglobulin-like domains of E-cadherin bond neighboring cells through junctional complexes (12, 13). To preserve cellular shape and polarity, the intracellular domains of cadherins connect to the actin cytoskeleton through α-catenin and β-catenin (14). Downregulation of E-cadherin in cancer cells is a critical disruptor of epithelial homeostasis, augmenting cell invasiveness (8, 12, 15). A "cadherin switch" has been described, whereby E-cadherin loss is accompanied by gain of N-cadherin (16), a mesenchymal marker (17). The molecular mechanisms of this switch are not known (18).

Loss of E-cadherin during cancer progression is regulated genetically and epigenetically. Promoter hypermethylation in breast cancer cells downregulates E-cadherin expression (19). Genetic mechanisms involve transcriptional repression at Ets sites or palindromic E-boxes (20) by repressors, such as the zinc-finger domain–containing factors *Snail, Slug, Zeb1*, and *Zeb2* and the basic helix-loop-helix factors *E47* and *Twist* (21, 22). Their function is regulated by oncogenic pathways, particularly by *ras* (23), *Src* (24), *Akt* (25), *GSK-3β* (26), and *NF-κB* (27). Integrin signaling triggered by anchoring of cancer cells in the ECM activates integrin-linked kinase (*ILK*; refs. 28, 29), which regulates E-cadherin function and the assembly of actin filaments by modulating the balance between *Rho* and *Rac* (28).

Given the role of TG2 in cell adhesion modulated by β-integrins (1, 30) and its role in activating oncogenic signaling (2), we speculated that it may be involved in EMT. Here we show that ovarian cancer cells expressing TG2 adopt a mesenchymal phenotype, characterized by cadherin switch and invasive behavior in a Matrigel matrix. TG2 modulates E-cadherin loss at the transcriptional level by altering the expression of several repressors including *Zeb1*. This function is mediated through activation of the NF-κB complex by TG2. We show by using an orthotopic xenograft ovarian model that TG2-dependent induction of EMT leads to increased tumor formation, peritoneal metastases, and malignant ascites.

Materials and Methods

Cell lines. Human SKOV3 and OV90 ovarian cancer cell lines from the American Type Culture Collection were cultured in growth medium containing 1:1 MCDB 105 (Sigma) and M199 (Cellgro) supplemented with 10% fetal bovine serum (Cellgro) and 1% antibiotics.

Note: Supplementary data for this article are available at Cancer Research Online (http://cancerres.aacrjournals.org/).

M. Shao and L. Cao contributed equally to this work.

Requests for reprints: Daniela Matei, IU Simon Cancer Center, 535 Barnhill Drive, RT 473, Indianapolis, IN 46202. Phone: 317-278-8844; Fax: 317-278-0074; E-mail: dmatei@iupui.edu.

doi:10.1158/0008-5472.CAN-09-1257

Published OnlineFirst December 1, 2009; DOI: 10.1158/0008-5472.CAN-09-1257

Transfection. To knock down TG2, an antisense construct (AS-TG2; ref. 31) cloned into pcDNA3.1 was transfected in SKOV3 cells, and stable clones were selected, as previously described (1). To overexpress TG2, TG2 subcloned in pQCXIP was transduced into OV90 cells, and stably expressing pooled colonies were selected, as described (7). To overexpress *Zeb1* and reconstitute NF-κB and Akt activities in SKOV3 cells stably transfected with AS-TG2 or vector, full-length *Zeb1* cDNA, constitutively active p65 subunit of NF-κB, and a constitutively active form of *Akt* that lacks the pleckstrin homology domain were transferred by retroviral infection and pooled colonies were selected. These vectors were previously described (27). Transfection of short interfering RNA (siRNA) was done using Dreamfect (Oz Biosciences) and siRNA targeting *Zeb1* (Dharmacon) or scrambled siRNA (control).

Western blotting. Cells were lysed in radioimmunoprecipitation assay buffer containing protease inhibitors. Equal amounts of protein were separated by SDS-PAGE and electroblotted onto polyvinylidene difluoride membranes (Millipore). After blocking, membranes were probed with primary antibodies against TG2 (Neomarkers), glyceraldehyde-3-phosphate dehydrogenase (GAPDH; Biodesign International), Zeb1 (Santa Cruz), E-cadherin (Cell Signaling), N-cadherin (Cell Signaling), and vimentin (Sigma). After incubation with horseradish peroxidase–conjugated secondary antibodies, antigen-antibody complexes were visualized using enhanced chemiluminescence (Amersham Biosciences). Images were captured with an image analyzer (LAS 3000, Fuji Film) and densitometry analysis was done with MultiGauge 3.0 software (Fujifilm USA, Inc.). Western blots were repeated in independent conditions at least twice; representative blots are shown.

Orthotopic ovarian xenograft model. SKOV3 cells stably transfected with AS-TG2 or vector (pcDNA3.1) were injected orthotopically under the ovarian bursa of 7- to 8-wk-old female nude mice (nu/nu BALB/c) from Harlan. For the orthotopic injection, mice were anesthetized with a cocktail of acepromazine and Torbugesic, and a dorsal incision exposed the left ovary enshrouded in its oviductal fimbriae. Using a 27-gauge needle attached to a piece of polyethylene tubing (PE-20) and held in place with a micromanipulator, 1.0×10^6 cells diluted in 5 μL of growth medium were injected into the ovarian bursa. Eight weeks after the injection, mice were euthanized and necropsy was done. In this first experiment, the SKOV3-pcDNA3.1 and SKOV3/AS-TG2 cells induced ovarian tumors but did not produce metastases. To produce a more aggressive phenotype, tumors were minced, treated with hyaluronidase, and cultured in medium supplemented with G418. Resultant xenograft-derived cell lines, SKOV3-pcDNA3.1× and SKOV3-AS-TG2×, were used in subsequent experiments.

Ovarian tumors were measured bidimensionally with calipers, and tumor volume was calculated as $L \times W^2/2$, where L is length and W is width. Peritoneal milliary seeding was estimated based on the presence of >10 disseminated nodules (yes/no), and peritoneal metastatic implants were counted. Because the primary goal was assessment of metastasis, animals that did not develop tumors within the ovary or that had discernable leakage at the time of injection were excluded from analysis. Four independent rounds of injection were done, with 10 to 11 mice being used each time. Results of these four rounds were analyzed and are presented together. Animal experiments were approved by the Indiana University Animal Care and Use Committee as being in compliance with federal regulations.

Matrigel invasion assay. Invasion assay was done by using two-dimensional and three-dimensional cell cultures in a Matrigel matrix (BD-Biosciences). Briefly, 2.5×10^4 cells suspended in 50 μL of cell culture medium were seeded onto solidified Matrigel in 24-well plates as a monolayer (two-dimensional model) or mixed and embedded within the matrix (three-dimensional model). After incubation at 37°C, invasive cells adhered to the surface of the gel and spread to form networks (two-dimensional model) or degraded and invaded into the gel (three-dimensional). These were observed under an inverted microscope and photographed live. The experiments were done in duplicate and repeated in independent conditions.

Gene reporter assays. Dual-Luciferase Assay (Promega) was done to quantify E-cadherin promoter activity in pcDNA3.1 and AS-TG2 SKOV3 cells. In brief, cells were transiently cotransfected with the experimental reporter plasmid, E-cadherin promoter firefly luciferase, containing the first 500 nucleotides and four E-box elements (32), and control reporter plasmid, cytomegalovirus promoter Renilla luciferase, at a ratio of 10:1 by using DreamFect Gold reagent (OZ Biosciences). Luminescence was measured by using a TD-20/20 luminometer (Turner Biosystems). Experiments were done in triplicate and repeated. To control for transfection efficiency, values for luminescence were normalized to Renilla activity.

Immunohistochemistry. Tumors harvested 8 wk after orthotopic injection were examined by immunohistochemistry for TG2, as described (1). For E-cadherin, a monoclonal antibody at 1:100 concentration (DAKO) and the avidin-biotin peroxidase system (DAKO) were used. Negative controls were run in parallel. Slides were scored from 0 to 3+, noting the percentage of staining cells, by a pathologist blinded to the identity of the samples.

Reverse transcription-PCR. RNA extracted by using the RNA STAT-60 reagent (Tel-Test, Inc.) was reverse-transcribed using the iScript cDNA synthesis kit (Bio-Rad). The PCR reactions used Taq polymerase (Promega) and the primers are described in Supplementary Table S1. For real-time PCR, we used the FastStart TaqMan Probe Master (Rox, Roche) on an ABI Prism 7900 platform (Applied Biosystems) according to the manufacturer's procedures. The primers and probes used are given in Supplementary Table S2. At the end of the PCR reaction, a melting curve was generated and the cycle threshold (C_t) was recorded for the reference gene and for GAPDH. Relative expression of gene of interest was calculated as ΔC_t, measured by subtracting the C_t of the reference gene from that of the control. Results are presented as mean ± SD of replicates. Each experiment was done in duplicate and repeated in independent conditions.

Immunofluorescence. SKOV3 cells plated on fibronectin-coated chamber slides (BD Biosciences) were fixed in 4% paraformaldehyde and permeabilized with Triton X-100. After blocking, cells were incubated with primary antibodies, anti–E-cadherin (1:200), Cy5-labeled anti-vimentin (Sigma, 1:200), and isotype-specific IgG (control), followed by incubation with Alexa Fluor 488–labeled secondary antibody (1:1,000; Molecular Probes). Images were captured using a Zeiss LSM 510 confocal microscope system under UV excitation at 488 nm (Alexa Fluor 488), 630 nm (Cy5), and 340 nm [4′,6-diamidino-2-phenylindole (DAPI)].

Statistical analysis. Fisher's exact test was used to compare metastasis and ascites formation and intensity of E-cadherin expression between experimental groups. Student's t test compared mean tumor volumes, relative luciferase activity, and mRNA expression levels between groups. A P value of <0.05 was deemed significant. We estimated the Pearson correlation coefficient between mRNA expression levels for TG2 and E-cadherin repressors, *Zeb1* and *Zeb2, Twist1* and *Twist2*, and *Slug* and *Snail1*, by using the data downloaded from GEO[7] (33). One-sample t test was used to test the hypothesis that the Pearson correlation coefficient is equal to zero.

Results

TG2 induces EMT in ovarian cancer cells. Having previously shown that TG2 enhances i.p. tumor dissemination (1, 34), we sought to determine whether the enzyme plays a role in EMT. We used two ovarian cancer cell lines, one expressing endogenous TG2 (SKOV3) and one lacking TG2 expression (OV90). SKOV3 cells were stably transfected with an antisense TG2 construct (AS-TG2) or control vector (pcDNA3.1), and OV90 cells were stably transduced with full-length TG2 or control vector (pQCXIP). Decreased expression level of TG2 in AS-TG2 cells compared with vector-transfected cells was shown by Western blotting (Fig. 1*A, top left*). Control cells expressing endogenous TG2 displayed poorly organized adhesive junctions and loss of cell polarity and exhibited a fibroblast-like morphology. In contrast, cells stably transfected with AS-TG2 appeared compact, flat, and cohesive (Fig. 1*A, top right*). A similar difference in phenotype was noted in OV90 cells

[7] http://www.ncbi.nlm.nih.gov/geo/

Published OnlineFirst December 1, 2009; DOI: 10.1158/0008-5472.CAN-09-1257

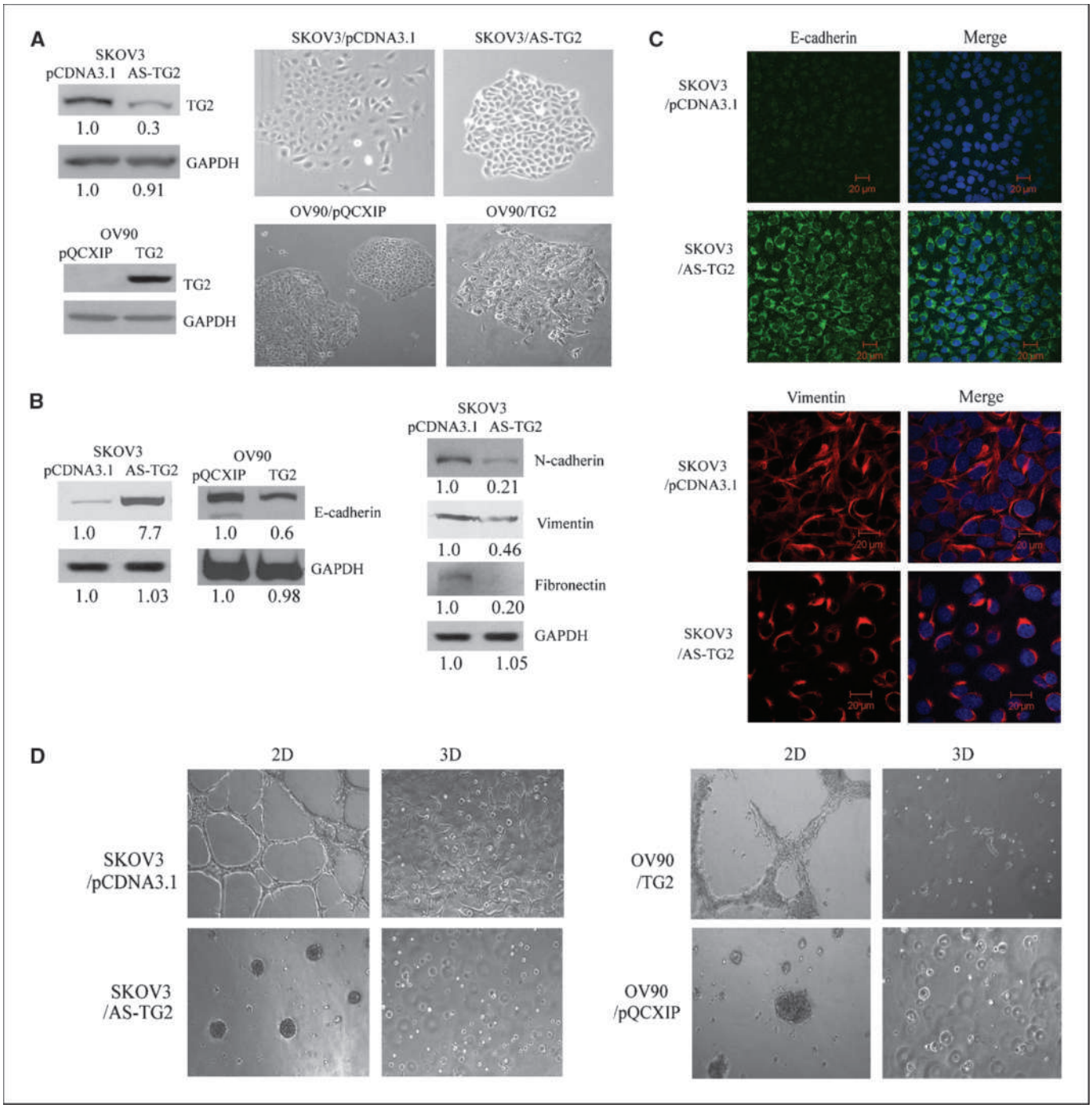

Figure 1. TG2 induces EMT in ovarian cancer cells. *A,* Western blotting for TG2 and GAPDH in vector- and AS-TG2–transfected SKOV3 cells (*top left*). Cell morphology of vector- and AS-TG2–transfected SKOV3 cells (*top right*; ×100 magnification). Western blotting for TG2 and GAPDH in vector- and TG2-transduced OV90 cells (*bottom left*). Cell morphology of vector and TG2 OV90 cells (*bottom right*; ×100 magnification). *B,* Western blotting for E-cadherin and GAPDH in vector- and AS-TG2–transfected SKOV3 cells (*left*) and in vector- and TG2-transduced OV90 cells (*middle*). Western blotting for other EMT markers, N-cadherin, vimentin, and fibronectin, in control and AS-TG2 cells (*right*). Densitometry quantifies the expression levels of E-cadherin, N-cadherin, vimentin, fibronectin, and TG2 relative to GAPDH. *C,* immunofluorescent staining for E-cadherin and vimentin in control and AS-TG2–transfected SKOV3 cells. Nuclei are visualized by DAPI staining. *D,* invasion through Matrigel using two-dimensional (*2D*) and three-dimensional (*3D*) cultures using SKOV3-pcDNA3.1 and AS-TG2 cells (*left*; ×100 magnification) or OV90-pQCXIP and TG2 cells (*right*; ×100 magnification).

with or without TG2 overexpression. Increased expression level of TG2 in TG2-transduced compared with vector-transduced OV90 cells was shown by Western blotting (Fig. 1*B, bottom left*). pQCXIP-transduced cells are compact and organized in tight structures, whereas TG2-transduced cells are elongated and dispersed (Fig. 1*B, bottom right*). These observations suggest that increased TG2 expression was associated with a mesenchymal morphology.

To confirm this, we examined the expression of E-cadherin and other EMT markers in cells engineered to express variable levels of TG2. A significant increase in E-cadherin expression was observed

Published OnlineFirst December 1, 2009; DOI: 10.1158/0008-5472.CAN-09-1257

in AS-TG2 compared with control cells (Fig. 1*B, left*). Correspondingly, decreased E-cadherin expression was noted in OV90 cells transduced with TG2 compared with control cells (Fig. 1*B, middle*). Knockdown of TG2 in SKOV3 cells was associated with a cadherin switch characterized by increased E-cadherin expression and decreased N-cadherin expression compared with control cells. Expression levels of other mesenchymal markers (fibronectin and vimentin) were decreased in cells transfected with AS-TG2 compared with control cells (Fig. 1*B, right*). This phenotype was confirmed by immunofluorescent staining. SKOV3 control cells dimly expressed E-cadherin and strongly stained with a vimentin antibody. In contrast, E-cadherin expression was increased and vimentin staining was diminished in AS-TG2 cells (Fig. 1*C*).

EMT renders cells motile and invasive. We next examined whether the mesenchymal morphology observed in TG2-expressing cells is associated with invasiveness. For this, cells were plated in two-dimensional and three-dimensional cultures in Matrigel matrix. SKOV3 cells transfected with vector formed networks in Matrigel, whereas AS-TG2 cells remained clumped together (Fig. 1*D*). Likewise, OV90 cells transduced with TG2 invaded through the matrix as trabecullae, whereas vector-transduced OV90 cells grew in cohesive, noninvading clumps (Fig. 1*D*). These results show that TG2 promotes EMT and invasiveness of ovarian cancer cells.

TG2 enhances ovarian tumor metastasis. The process of EMT is linked to initiation of metastasis. We previously showed that TG2 enhances i.p. tumor dissemination (1). However, the i.p. model artificially dispersed ovarian cancer cells in the peritoneal cavity and did not appreciate the first steps of metastasis, specifically invasion and shedding of cells from the ovary. To overcome these limitations, here we used an orthotopic ovarian xenograft model, where control and AS-TG2–transfected SKOV3 cells were injected into the ovarian bursa of nude mice.

In an initial experiment, necropsies were done 8 weeks after ovarian cancer cell implantation. Primary ovarian tumors were formed in mice injected with either AS-TG2 or control cells and

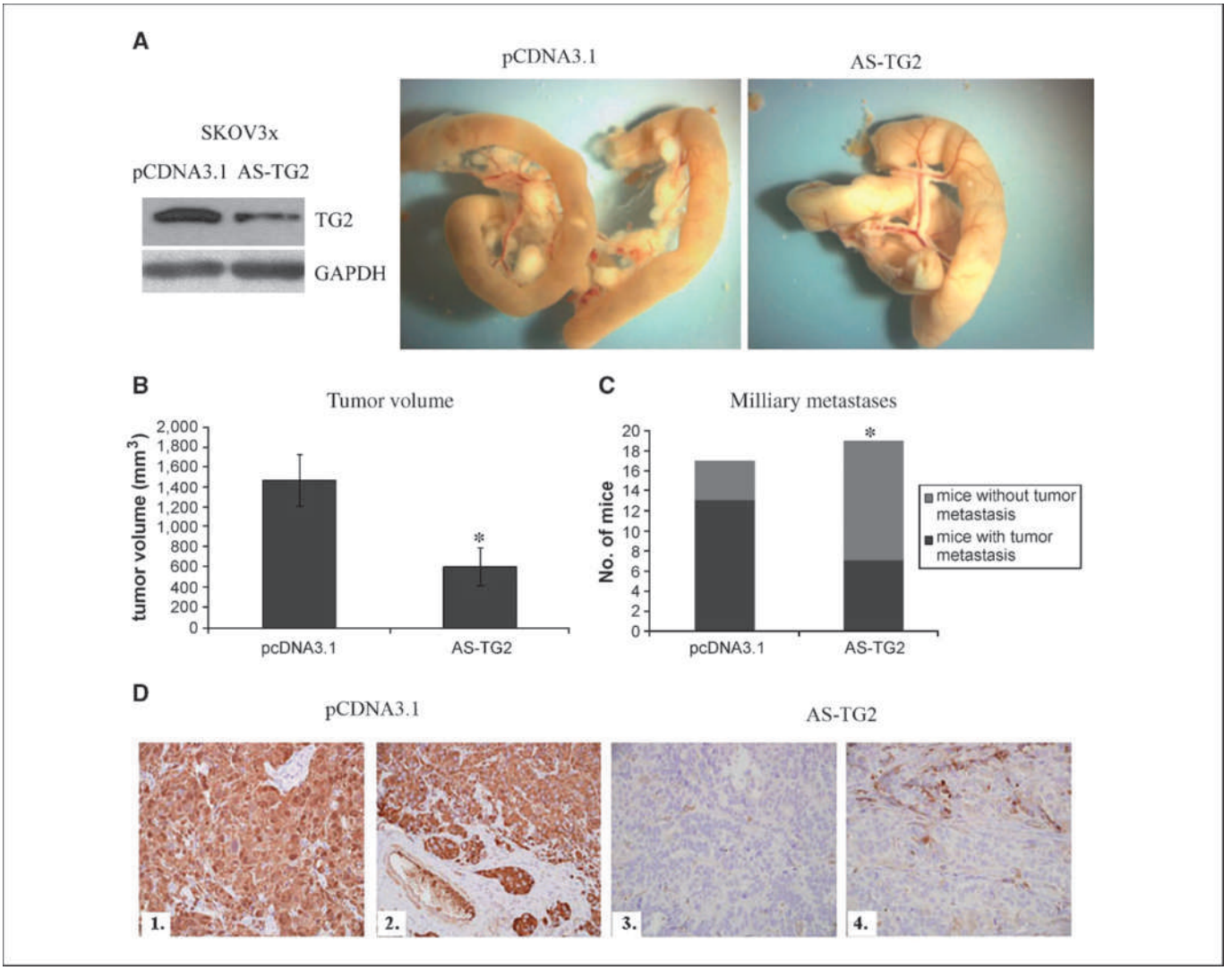

Figure 2. TG2 knockdown suppresses tumor metastasis in an ovarian cancer orthotopic xenograft model. *A,* Western blotting for TG2 in xenograft-derived cells (*left*). Mice injected with pcDNA3.1× formed tumors studding the mesentery adjacent to the small bowel, whereas mice injected with AS-TG2× cells had clear mesentery and bowel (*right*). *B,* comparison of mean tumor volumes from mice implanted with pcDNA3.1× and AS-TG2× cells. *Columns,* mean tumor volumes; *bars,* SEM ($P = 0.01$). *C,* number of mice developing disseminated milliary metastases after pCDNA3.1× and AS-TG2× SKOV3 cell orthotopic implantation. *Columns,* number of mice ($P = 0.02$). *D,* immunohistochemistry for TG2 in tumors derived from pcDNA3.1× (*1, 2*) or AS-TG2× cells (*3, 4*).

Published OnlineFirst December 1, 2009; DOI: 10.1158/0008-5472.CAN-09-1257

Table 1. Tumor formation in the peritoneal space according to TG2 expression

	SKOV3-pCDNA3.1×	SKOV3-AS-TG2×	*P*
No. mice injected	21	22	—
No. mice that formed ovarian tumors	17	19	—
Volume of primary ovarian tumor (mm^3)	1,468 ± 257	600 ± 187	0.01*
No. mice with ascites	10	4	0.03*
No. mice with milliary spread	13	7	0.02*
No. implants	24 ± 5	9 ± 3	0.04*

*Statistically significant. Data is presented as average volume and average number of implants ± SEM.

their sizes were similar. However, no distant metastases or malignant ascites were generated (Supplementary Table S3). Knowing that the metastatic potential of tumor cells is enhanced through animal passaging, we used ovarian tumors harvested from this experiment to generate xenograft-derived cultures. Western blotting showed that the expression level of TG2 in xenograft-derived cells remained lower in AS-TG2 xenograft–derived cells (AS-TG2×) compared with pcDNA3.1 xenograft–derived cells (pCDNA3.1×; Fig. 2*A, left*). These cells, passaged once as ovarian xenografts, were used for a new round of orthotopic ovarian implantation. After 8 weeks, a significant difference in tumor development was observed (Fig. 2*A*; Table 1). The mean volume of primary tumors was significantly smaller in mice injected with AS-TG2× cells compared with that in mice injected with pcDNA3.1× cells (600 ± 187 versus 1,468 ± 257 mm^3; $P = 0.01$; Fig. 2*B*). Mice injected with pcDNA3.1× cells developed disseminated metastatic implants on the omentum, mesentery, and peritoneal surface of abdominal flanks compared with mice injected with AS-TG2× cells. Specifically, 13 of 17 mice injected with pcDNA3.1× cells developed disseminated milliary metastases [>10 implants; Fig. 2*A* (*middle*) and *C*], compared with 7 of 19 mice injected with AS-TG2× cells [$P = 0.02$; Fig. 2*A* (*right*) and *C*]. The average number of peritoneal implants in mice injected with control cells was 24 ± 5 and in mice injected with AS-TG2 cells was 9 ± 3 ($P = 0.04$; Table 1). Ascites formation was also different between the two groups, with 10 of 17 mice injected with pcDNA3.1× cells having developed ascites compared with 4 of 19 mice injected with AS-TG2× cells ($P = 0.038$; Table 1). TG2 expression was verified by immunohistochemistry. Suppressed TG2 expression was observed in tumors generated from AS-TG2× cells (Fig. 2*D, sections 3* and *4*) compared with tumors generated from pcDNA3.1× cells (Fig. 2*D, sections 1* and *2*). Occasional small and isolated islands of TG2-positive cells were observed in AS-TG2× tumors, consistent with the emergence of TG2-positive subpopulations in the absence of G418 selection *in vivo*.

To investigate the effects of TG2 on markers of EMT *in vivo*, E-cadherin expression was assessed by immunohistochemistry (Fig. 3*A*). Twelve of 16 tumor specimens derived from AS-TG2× cells stained strongly (2+ and 3+) for E-cadherin, compared with 5 of 18 pCDNA3.1× derived xenografts ($P = 0.015$; Fig. 3*B*). For few E-cadherin–positive pcDNA3.1× xenografts, available metastatic implants were immunostained. Distant implants displayed negative E-cadherin staining, consistent with the concept that E-cadherin is downregulated at metastatic sited compared with primary tumor sites (Supplementary Fig. S1). These data show that TG2-induced E-cadherin repression is maintained *in vivo*, inversely correlating with the metastatic potential of the xenografts.

TG2 negatively regulates E-cadherin at the transcription level by modulating the expression of transcription repressors. We next investigated the mechanisms of E-cadherin repression by TG2. Reverse transcription-PCR (RT-PCR) showed that E-cadherin mRNA level was upregulated in AS-TG2 cells compared

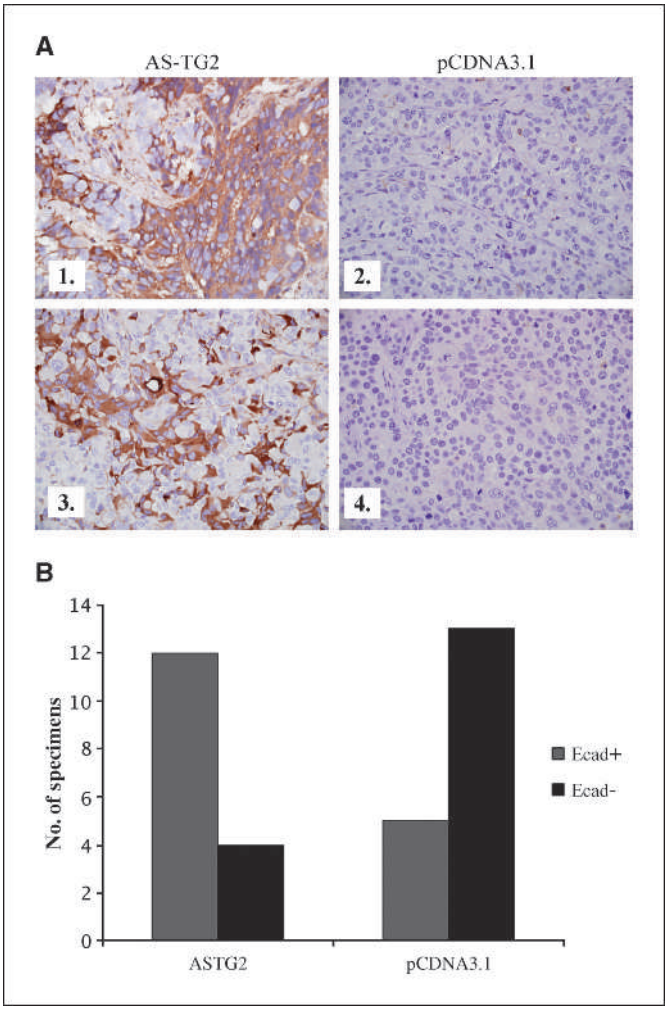

Figure 3. Immunohistochemistry for E-cadherin in xenografts derived from AS-TG2× and pcDNA3.1× cells. *A*, strong E-cadherin staining in AS-TG2× tumor specimens (*sections 1* and *3*) compared with pcDNA3.1× tumor specimens (*sections 2* and *4*). *B*, number of E-cadherin positive (2+ and 3+) and negative (0 and 1+) tumor specimens derived from AS-TG2× and pcDNA3.1× cells ($P = 0.015$).

Published OnlineFirst December 1, 2009; DOI: 10.1158/0008-5472.CAN-09-1257

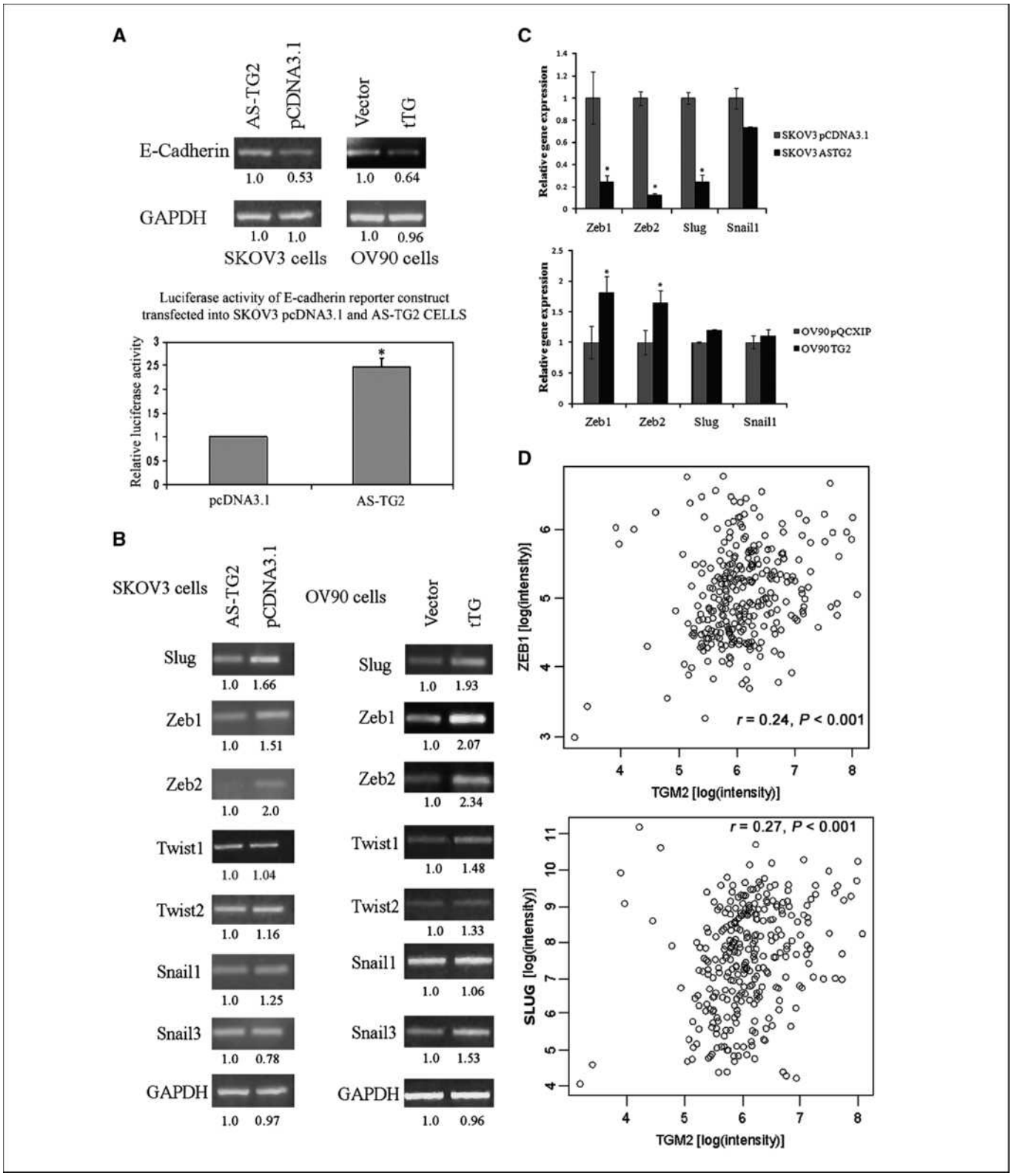

Figure 4. TG2 negatively regulates E-cadherin at the transcriptional level. *A,* semiquantitative RT-PCR for E-cadherin and GAPDH in SKOV3 control and AS-TG2 cells (*top left*) and in vector- and TG2-transduced OV90 cells (*top right*). A gene reporter assay of E-cadherin promoter activity in AS-TG2 and pcDNA3.1 SKOV3 cells, conducted as described in Materials and Methods (*bottom*). *Columns,* mean fold difference based on duplicate measurements; *bars,* SEM ($P < 0.001$). *B,* semiquantitative RT-PCR for E-cadherin transcriptional repressors in pcDNA3.1 and AS-TG2 SKOV3 cells (*left*) and pQCXIP- and TG2-transduced OV90 cells (*right*). Densitometry quantifies the level of expression of E-cadherin repressors relative to GAPDH. *C,* quantitative PCR for *Zeb1, Zeb2, Slug*, and *Snail1* in SKOV3 cells transfected with AS-TG2 or vector (*top*) and in OV90 cells transduced with TG2 or vector (*bottom*). *Columns,* mean of duplicate measurements; *bars,* SD. *, $P < 0.05$. *D,* correlation between *TG2* and *Zeb1* mRNA expression levels in human ovarian tumors (*top*). Correlation between *TG2* and *Slug* mRNA expression levels in human ovarian tumors (*bottom*). *X* and *Y axes,* signal intensity level measured by cDNA microarrays and expressed at the natural logarithm scale.

Published OnlineFirst December 1, 2009; DOI: 10.1158/0008-5472.CAN-09-1257

with control cells (Fig. 4*A*). In contrast, E-cadherin mRNA level was downregulated in OV90 cells transduced with TG2 compared with vector-transduced cells (Fig. 4*A*). A gene reporter assay in which AS-TG2 and control cells were transfected with an *E-cadherin*-luciferase reporter construct (32) showed that its reporter activity was increased 2.6-fold by TG2 knockdown (Fig. 4*A, bottom*; $P < 0.001$). These data show that TG2 negatively regulates *E-cadherin* at the transcriptional level.

Several transcriptional repressors are recognized as critical modulators of EMT, including *Snail, Slug, Zeb1, Zeb2*, and *Twist* (21, 22, 35, 36). To find out whether TG2 expression is associated with altered mRNA expression of these repressors, semiquantitative RT-PCR and real-time PCR were used. Diminished mRNA expression levels for *Slug, Zeb1*, and *Zeb2*, but not for *Twist1, Twist2, Snail1*, and *Snail 3*, were observed in AS-TG2 compared with control cells (Fig. 4*B, left*). Real-time PCR showed that *Zeb1, Zeb2*, and *Slug* mRNA expression levels were decreased by ~80% in AS-TG2–transfected cells compared with controls, but that *Snail1* expression level was not significantly different between the two cell types (Fig. 4*C, top*). Similar trends were observed in OV90 cells. *Slug, Zeb1*, and *Zeb2* mRNA levels were increased in OV90-TG2 compared with control cells. In addition, *Twist1* and *Snail 3* mRNA levels were slightly upregulated in TG2-overexpressing cells (Fig. 4*B, right*). Real-time PCR confirmed a 75% increase in mRNA expression level for *Zeb1* and *Zeb2* in OV90-TG2 compared with control cells, but no significant difference for *Slug* and *Snail1* (Fig. 4*C, bottom*). These data suggest that in ovarian cancer cells, TG2 expression correlates with expression of *E-cadherin* transcriptional repressors, particularly with that of *Zeb1* and *Zeb2*.

Next, we investigated in human tumors the correlation between expression of TG2 and that of E-cadherin repressors by using an existing database derived from microarray gene expression analysis of 285 ovarian tumors (37). Statistically significant correlations were found between *TG2* and *Zeb1* (Pearson correlation coefficient = 0.24, $P < 0.001$; see Fig. 4*D*), between *TG2* and *Slug* (Pearson correlation coefficient = 0.27, $P < 0.001$; see Fig. 4*D*), and, to a lesser degree, between *TG2* and *Snail2* (Pearson correlation coefficient = 0.14, $P = 0.02$). TG2 mRNA expression level did not correlate with that of *Twist1, Twist2*, or *Zeb2* in this database (Supplementary Table S4).

Based on these results and on a recent report implicating *Zeb1* in ovarian epithelial cell transformation (38), we focused on the effects of *TG2* on *Zeb1*. *Zeb1* expression was confirmed at the protein level. Consistent with RT-PCR data, lower *Zeb1* expression was observed in AS-TG2 compared with control cells (Fig. 5*A, left*). To test whether *Zeb1* negatively regulates E-cadherin in ovarian cancer cells, we used siRNA targeting *Zeb1*. E-cadherin expression level was upregulated in SKOV3 cells transfected with *Zeb1* siRNA compared with cells transfected with control siRNA (Fig. 5*A, right*).

To show the significance of *Zeb1* to regulation of E-cadherin expression by TG2, we stably overexpressed *Zeb1* in SKOV3 cells where TG2 was knocked down. The expression level of E-cadherin, which was markedly increased by TG2 knockdown compared with control cells (Fig. 5*B, left, lane 2* versus *lane 1*), was reduced significantly by overexpression of *Zeb1* (Fig. 5*B, left, lane 3* versus *lane 2*). Overexpression of *Zeb1* in cells with decreased expression of TG2 led to restoration of the invasive phenotype, comparable to that of cells expressing TG2, as assessed by a two- or three-dimensional Matrigel invasion assay (Fig. 5*B, right*). These data suggest that *Zeb1* plays a critical role in TG2-mediated regulation of *E-cadherin* expression and the invasive phenotype of ovarian cancer cells.

Given the role of TG2 in activating the NF-κB complex and Akt (2, 34), and the known functions of these pathways in modulating EMT (25, 27), we investigated whether the effects of TG2 on *Zeb1* and EMT are induced as a consequence of Akt or NF-κB activation. To test this, we overexpressed the p65 subunit of NF-κB or a constitutively active form of Akt (CA-Akt) in ovarian cancer cells where TG2 was knocked down and compared the expression levels of *Zeb1* and *E-cadherin* to those in cells expressing endogenous TG2. Overexpression of p65 in AS-TG2 cells was confirmed by Western blotting for IκBα (Fig. 5*C, left*) and overexpression of CA-Akt was verified by Western blotting for Akt (Fig. 5*C, middle*). *Zeb1* expression level was lower in AS-TG2 cells compared with control cells, and this corresponded to increased E-cadherin expression level (Fig. 5*C, right, lane 2* versus *lane 1*). Overexpression of p65 in AS-TG2 cells rescued *Zeb1* expression level, repressing in turn E-cadherin level (Fig. 5*C, right, lane 3* versus *lane 2*). As assessed by a Matrigel invasion assay, overexpression of p65 in AS-TG2 cells led to an invasive phenotype comparable to that of control cells (Fig. 5*D*), suggesting that an important element in the process of TG2-induced EMT is the repressor *Zeb1* induced by NF-κB. Overexpression of CA-Akt in AS-TG2 cells also repressed E-cadherin level (Fig. 5*C, right, lane 4* versus *lane 2*) and induced an invasive phenotype (Fig. 5*D*). However, CA-Akt overexpression did not affect *Zeb1* (Fig. 5*C, left, lane 4* versus *lane 2*), suggesting that other mechanisms are implicated downstream of Akt. Collectively, these data indicate that TG2 negatively regulates E-cadherin expression, leading to EMT, increased cancer cell invasiveness, and metastasis.

Discussion

We previously showed that TG2 plays a role in peritoneal dissemination of ovarian tumors (1). In the current study, we provide strong evidence for its role in metastasis and present novel mechanistic insight into how TG2 facilitates tumor spread. We show that TG2 induces a mesenchymal phenotype and that this, in turn, translates into increased cell invasiveness and tumor metastasis. This is mediated by TG2 through effects on transcriptional repressors that regulate E-cadherin expression. To our knowledge, this is the first report implicating TG2 in EMT and establishes a critical link between the enzyme, cancer cell invasion, and metastasis.

Several oncogenic signal transduction pathways have been implicated in regulating E-cadherin expression in cancer cells (25, 27, 39). For instance, the NF-κB pathway, constitutively activated in many epithelial tumors, induces EMT by regulating the function of the *Zeb* family of transcription factors (27). Recent reports implicate *Zeb1* and *Zeb2* in mesenchymal transformation of ovarian cancer cells under the control of microRNA 200 (40). The results presented here point to *Zeb1* as an important EMT regulator, downstream of TG2 and of the activated NF-κB complex. We recognize that other mechanisms may be recruited by TG2 to repress E-cadherin expression. A potential pathway may be activation of the serine/threonine kinase *Akt* by TG2 (6). It has been shown that *Akt* represses E-cadherin transcription by stabilizing the function of the repressors *Snail* and *Slug* (25), and it is possible that a similar mechanism may operate in ovarian cancer cells.

Aside from the general implications of EMT in tumor progression (8), there are specific nuances about EMT in ovarian cancer. It has been suggested that after shedding from the primary site, ovarian cancer cells float in the peritoneal cavity as cell aggregates or spheroids (33). Within spheroid structures, cells adopt a mesenchymal phenotype (33, 41) that is closely regulated by cytokines and

Published OnlineFirst December 1, 2009; DOI: 10.1158/0008-5472.CAN-09-1257

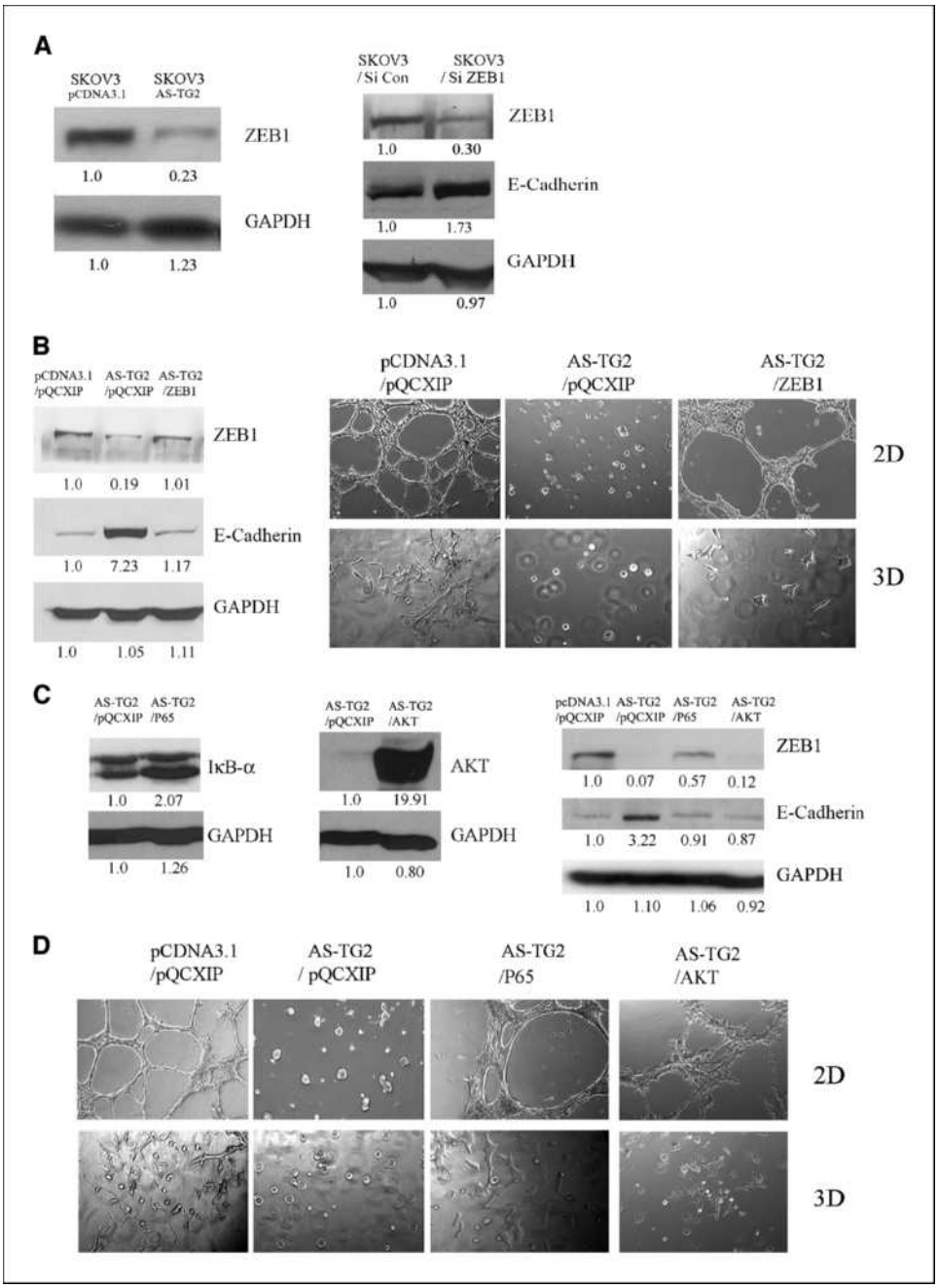

Figure 5. TG2 regulates E-cadherin expression by modulating Zeb1. *A,* Western blotting for Zeb1 in pcDNA3.1- and AS-TG2–transfected SKOV3 cells (*left*) and Western blotting for Zeb1 and E-cadherin in SKOV3 cells transfected with siRNA targeting *Zeb1* or with control siRNA (*right*). Densitometry quantifies Zeb1 expression relative to GAPDH. *B, left,* Western blotting for Zeb1 and E-cadherin in SKOV3 cells transfected with pcDNA3.1 or AS-TG2 and transduced with *Zeb1* or pQCXIP. *Right,* invasion through Matrigel of SKOV3-pcDNA3.1 and AS-TG2 cells transduced with pQCXIP or *Zeb1* (×100). *C, left,* Western blotting for IκBα of AS-TG2 cells transduced with pQCXIP or p65. *Middle,* Western blotting for Akt of AS-TG2 cells transduced with pQCXIP or CA-Akt. *Right,* Western blotting for Zeb1, E-cadherin, and GAPDH of SKOV3 cells transfected with pcDNA3.1 or AS-TG2 and transduced with pQCXIP, p65, or CA-Akt. Densitometry quantifies the expression levels for Zeb1 and E-cadherin relative to GAPDH. *D,* invasion through Matrigel of SKOV3-pcDNA3.1 and AS-TG2 cells transduced with pQCXIP, p65, or CA-Akt (×100).

the peritoneal hormonal milieu. Such influences may include regulation by estrogen (42) or transforming growth factor β (38), secreted in the peritoneal fluid. The mesenchymal phenotype allows cells within spheroids to become invasive when in contact with the mesothelium (41). We observed decreased spheroid formation by AS-TG2 cells compared with control cells in nonadherent culture conditions (not shown) supporting this function. Mesenchymal transformation of epithelial ovarian cells also increases secretion of MMPs (43), which remodel the ECM (44). Digestion of ECM by MMPs is critical to establishment of metastases and sprouting of new vessels. Recent data from our laboratory showed that TG2 regulates MMP-2 secretion by ovarian cancer cells (7). Those data in concert with the present findings support a critical role of the enzyme in regulating the invasiveness of ovarian cancer cells.

The use of orthotopic ovarian xenografts rather than i.p. tumor implantation (1) provides stronger evidence for the role of TG2 in metastasis. The orthotopic approach better mimics the phenomena of primary tumor formation and of tumor spreading initiated from the primary site. Critical steps of this process are invasion outside of the ovarian bursa followed by i.p. dissemination with invasion of the mesothelium, which cannot be appreciated with i.p. xenografts (45, 46). Previous studies using orthotopic ovarian models used either implantation of human (46) or murine (47) tumor fragments adjacent to the ovary or injection of cancer cell lines under the ovarian bursa (45). The approach using tumor fragments microsurgically sutured to the oviductal fimbriae cannot appreciate invasion of cells out of the bursa into the peritoneal space. Intrabursal injection of ovarian cancer cells causes tumor

Published OnlineFirst December 1, 2009; DOI: 10.1158/0008-5472.CAN-09-1257

formation in the ovary; however, invasion and peritoneal spreading may not occur (45). In our first experiment, SKOV3 cells injected intrabursally formed large ovarian tumors but did not cause peritoneal dissemination. After only one passage as xenografts, cells injected intrabursally led to omental and mesenteric metastases. Passaging of cell lines as xenografts permits selection of more invasive cells with increased tumorigenicity (48). The orthotopic ovarian model using the animal-passaged cancer cells described here accurately reconstitutes primary tumor formation in the ovary followed by peritoneal dissemination after invasion through the bursa, recapitulating the steps of metastasis observed during the progression of ovarian cancer.

We show, using this model, that TG2 knockdown decreases tumor growth and peritoneal dissemination. The current findings are concordant with our previous results (1) and with a report showing a strong association between TG2 expression and adverse clinical outcome in ovarian cancer (49). The proinvasive and metastatic functions of TG2 may be specific to particular epithelial cancer types [e.g., pancreatic (50) and ovarian (1) cancers] that rely on peritoneal dissemination. The EMT phenotype has been also associated with chemotherapy resistance and may be implicated in TG2-mediated chemotherapy resistance reported by our group and by others (6, 34). Collectively, these data show that activation of oncogenic signaling by TG2 induces EMT and enhances tissue invasiveness and tumor dissemination.

Disclosure of Potential Conflicts of Interest

No potential conflicts of interest were disclosed.

Acknowledgments

Received 4/7/09; revised 9/21/09; accepted 10/14/09; published OnlineFirst 12/1/09.

Grant support: U.S. Department of Veterans Affairs through a VA Merit Award (D. Matei).

The costs of publication of this article were defrayed in part by the payment of page charges. This article must therefore be hereby marked *advertisement* in accordance with 18 U.S.C. Section 1734 solely to indicate this fact.

We thank Drs. Tucholski (University of Alabama, Birmingham, AL) and Martignetti and Difeo (Mount Sinai Medical School, New York, NY) for the constructs, and Drs. Kenneth Nephew, Mircea Ivan, and David Donner for careful review of the manuscript.

References

1. Satpathy M, Cao L, Pincheira R, et al. Enhanced peritoneal ovarian tumor dissemination by tissue transglutaminase. Cancer Res 2007;67:7194–202.
2. Mann AP, Verma A, Sethi G, et al. Overexpression of tissue transglutaminase leads to constitutive activation of nuclear factor-κB in cancer cells: delineation of a novel pathway. Cancer Res 2006;66:8788–95.
3. Pincus JH, Waelsch H. The specificity of transglutaminase. II. Structural requirements of the amine substrate. Arch Biochem Biophys 1968;126:44–52.
4. Matei D, Graeber TG, Baldwin RL, Karlan BY, Rao J, Chang DD. Gene expression in epithelial ovarian carcinoma. Oncogene 2002;21:6289–98.
5. Fesus L, Piacentini M. Transglutaminase 2: an enigmatic enzyme with diverse functions. Trends Biochem Sci 2002;27:534–9.
6. Verma A, Guha S, Wang H, et al. Tissue transglutaminase regulates focal adhesion kinase/AKT activation by modulating PTEN expression in pancreatic cancer cells. Clin Cancer Res 2008;14:1997–2005.
7. Satpathy M, Shao M, Emerson R, Donner DB, Matei D. Tissue transglutaminase regulates MMP-2 in ovarian cancer by modulating CREB activity. J Biol Chem 2009; 284:15390–9.
8. Thiery JP. Epithelial-mesenchymal transitions in tumour progression. Nat Rev Cancer 2002;2:442–54.
9. Yamashita S, Miyagi C, Fukada T, Kagara N, Che YS, Hirano T. Zinc transporter LIVI controls epithelial-mesenchymal transition in zebrafish gastrula organizer. Nature 2004;429:298–302.
10. Nagar B, Overduin M, Ikura M, Rini JM. Structural basis of calcium-induced E-cadherin rigidification and dimerization. Nature 1996;380:360–4.
11. Shapiro L, Fannon AM, Kwong PD, et al. Structural basis of cell-cell adhesion by cadherins. Nature 1995;374: 327–37.
12. Nagafuchi A, Shirayoshi Y, Okazaki K, Yasuda K, Takeichi M. Transformation of cell adhesion properties by exogenously introduced E-cadherin cDNA. Nature 1987;329:341–3.
13. Patel DJ, Gumbiner BM. Cell-cell recognition. Zipping together a cell adhesion interface. Nature 1995; 374:306–7.
14. Cavey M, Rauzi M, Lenne PF, Lecuit T. A two-tiered mechanism for stabilization and immobilization of E-cadherin. Nature 2008;453:751–6.
15. Perl AK, Wilgenbus P, Dahl U, Semb H, Christofori G. A causal role for E-cadherin in the transition from adenoma to carcinoma. Nature 1998;392:190–3.
16. Kuphal S, Bosserhoff AK. Influence of the cytoplasmic domain of E-cadherin on endogenous N-cadherin expression in malignant melanoma. Oncogene 2006;25: 248–59.
17. Kim JB, Islam S, Kim YJ, et al. N-Cadherin extracellular repeat 4 mediates epithelial to mesenchymal transition and increased motility. J Cell Biol 2000;151:1193–206.
18. Nieman MT, Prudoff RS, Johnson KR, Wheelock MJ. N-cadherin promotes motility in human breast cancer cells regardless of their E-cadherin expression. J Cell Biol 1999;147:631–44.
19. Graff JR, Herman JG, Lapidus RG, et al. E-cadherin expression is silenced by DNA hypermethylation in human breast and prostate carcinomas. Cancer Res 1995; 55:5195–9.
20. Hajra KM, Chen DY, Fearon ER. The SLUG zinc-finger protein represses E-cadherin in breast cancer. Cancer Res 2002;62:1613–8.
21. Moreno-Bueno G, Cubillo E, Sarrio D, et al. Genetic profiling of epithelial cells expressing E-cadherin repressors reveals a distinct role for Snail, Slug, and E47 factors in epithelial-mesenchymal transition. Cancer Res 2006;66:9543–56.
22. Peinado H, Olmeda D, Cano A. Snail, Zeb and bHLH factors in tumour progression: an alliance against the epithelial phenotype? Nat Rev Cancer 2007;7:415–28.
23. Boyer B, Roche S, Denoyelle M, Thiery JP. Src and Ras are involved in separate pathways in epithelial cell scattering. EMBO J 1997;16:5904–13.
24. Rodier JM, Valles AM, Denoyelle M, Thiery JP, Boyer B. pp60c-src is a positive regulator of growth factor-induced cell scattering in a rat bladder carcinoma cell line. J Cell Biol 1995;131:761–73.
25. Grille SJ, Bellacosa A, Upson J, et al. The protein kinase Akt induces epithelial mesenchymal transition and promotes enhanced motility and invasiveness of squamous cell carcinoma lines. Cancer Res 2003;63:2172–8.
26. Zhou BP, Deng J, Xia W, et al. Dual regulation of Snail by GSK-3β-mediated phosphorylation in control of epithelial-mesenchymal transition. Nat Cell Biol 2004;6: 931–40.
27. Chua HL, Bhat-Nakshatri P, Clare SE, Morimiya A, Badve S, Nakshatri H. NF-κB represses E-cadherin expression and enhances epithelial to mesenchymal transition of mammary epithelial cells: potential involvement of ZEB-1 and ZEB-2. Oncogene 2007;26: 711–24.
28. Fuchs BC, Fujii T, Dorfman JD, et al. Epithelial-to-mesenchymal transition and integrin-linked kinase mediate sensitivity to epidermal growth factor receptor inhibition in human hepatoma cells. Cancer Res 2008;68: 2391–9.
29. Li Y, Yang J, Dai C, Wu C, Liu Y. Role for integrin-linked kinase in mediating tubular epithelial to mesenchymal transition and renal interstitial fibrogenesis. J Clin Invest 2003;112:503–16.
30. Akimov SS, Krylov D, Fleischman LF, Belkin AM. Tissue transglutaminase is an integrin-binding adhesion coreceptor for fibronectin. J Cell Biol 2000;148:825–38.
31. Tucholski J, Lesort M, Johnson GV. Tissue transglutaminase is essential for neurite outgrowth in human neuroblastoma SH-SY5Y cells. Neuroscience 2001;102: 481–91.
32. DiFeo A, Narla G, Camacho-Vanegas O, et al. E-cadherin is a novel transcriptional target of the KLF6 tumor suppressor. Oncogene 2006;25:6026–31.
33. Sodek KL, Ringuette MJ, Brown TJ. Compact spheroid formation by ovarian cancer cells is associated with contractile behavior and an invasive phenotype. Int J Cancer 2008;124:2060–70.
34. Cao L, Petrusca DN, Satpathy M, Nakshatri H, Petrache I, Matei D. Tissue transglutaminase protects epithelial ovarian cancer cells from cisplatin induced apoptosis by promoting cell survival signaling. Carcinogenesis 2008;29:1893–900.
35. Julien S, Puig I, Caretti E, et al. Activation of NF-κB by Akt upregulates Snail expression and induces epithelium mesenchyme transition. Oncogene 2007;26:7445–56.
36. Olmeda D, Jorda M, Peinado H, Fabra A, Cano A. Snail silencing effectively suppresses tumour growth and invasiveness. Oncogene 2007;26:1862–74.
37. Tothill RW, Tinker AV, George J, et al. Novel molecular subtypes of serous and endometrioid ovarian cancer linked to clinical outcome. Clin Cancer Res 2008;14: 5198–208.
38. Hurt EM, Saykally JN, Anose BM, Kalli KR, Sanders MM. Expression of the ZEB1 (δEF1) transcription factor in human: additional insights. Mol Cell Biochem 2008; 318:89–99.
39. Cheng GZ, Chan J, Wang Q, Zhang W, Sun CD, Wang LH. Twist transcriptionally up-regulates AKT2 in breast cancer cells leading to increased migration, invasion, and resistance to paclitaxel. Cancer Res 2007;67:1979–87.

Published OnlineFirst December 1, 2009; DOI: 10.1158/0008-5472.CAN-09-1257

40. Park SM, Gaur AB, Lengyel E, Peter ME. The miR-200 family determines the epithelial phenotype of cancer cells by targeting the E-cadherin repressors ZEB1 and ZEB2. Genes Dev 2008;22:894–907.

41. Burleson KM, Hansen LK, Skubitz AP. Ovarian carcinoma spheroids disaggregate on type I collagen and invade live human mesothelial cell monolayers. Clin Exp Metastasis 2004;21:685–97.

42. Park SH, Cheung LW, Wong AS, Leung PC. Estrogen regulates Snail and Slug in the down-regulation of E-cadherin and induces metastatic potential of ovarian cancer cells through estrogen receptor α. Mol Endocrinol 2008;22:2085–98.

43. Ahmed N, Maines-Bandiera S, Quinn MA, Unger WG, Dedhar S, Auersperg N. Molecular pathways regulating EGF-induced epithelio-mesenchymal transition in human ovarian surface epithelium. Am J Physiol Cell Physiol 2006;290:C1532–42.

44. Duong TD, Erickson CA. MMP-2 plays an essential role in producing epithelial-mesenchymal transformations in the avian embryo. Dev Dyn 2004;229:42–53.

45. Shaw TJ, Senterman MK, Dawson K, Crane CA, Vanderhyden BC. Characterization of intraperitoneal, orthotopic, and metastatic xenograft models of human ovarian cancer. Mol Ther 2004;10:1032–42.

46. Fu X, Hoffman RM. Human ovarian carcinoma metastatic models constructed in nude mice by orthotopic transplantation of histologically-intact patient specimens. Anticancer Res 1993;13:283–6.

47. Sengupta S, Kim KS, Berk MP, et al. Lysophosphatidic acid downregulates tissue inhibitor of metalloproteinases, which are negatively involved in lysophosphatidic acid-induced cell invasion. Oncogene 2007;26:2894–901.

48. Tom BH, Rutzky LP, Oyasu R, Tomita JT, Goldenberg DM, Kahan BD. Human colon adenocarcinoma cells. II. Tumorigenic and organoid expression *in vivo* and *in vitro*. J Natl Cancer Inst 1977;58:1507–12.

49. Hwang JY, Mangala LS, Fok JY, et al. Clinical and biological significance of tissue transglutaminase in ovarian carcinoma. Cancer Res 2008;68:5849–58.

50. Verma A, Wang H, Manavathi B, et al. Increased expression of tissue transglutaminase in pancreatic ductal adenocarcinoma and its implications in drug resistance and metastasis. Cancer Res 2006;66:10525–33.

Cancer Research
The Journal of Cancer Research (1916–1930) | The American Journal of Cancer (1931–1940)

AACR American Association for Cancer Research

Epithelial-to-Mesenchymal Transition and Ovarian Tumor Progression Induced by Tissue Transglutaminase

Minghai Shao, Liyun Cao, Changyu Shen, et al.

Cancer Res 2009;69:9192-9201. Published OnlineFirst December 1, 2009.